Published in final edited form as:
FEBS Lett. 2014 May 2; 588(9): 1850–1856. doi:10.1016/j.febslet.2014.03.057.

MIR146A inhibits *JMJD3* expression and osteogenic differentiation in human mesenchymal stem cells

Jessica M. Huszar and **Christopher J. Payne**
Driskill Graduate Program, Departments of Pediatrics and Obstetrics and Gynecology, Northwestern University Feinberg School of Medicine and Human Molecular Genetics Program, Ann & Robert H. Lurie Children's Hospital of Chicago Research Center, Chicago, IL 60611, USA

Abstract

Chromatin remodeling is important for cell differentiation. Histone methyltransferase EZH2 and histone demethylase JMJD3 (KDM6B) modulate levels of histone H3 lysine 27 trimethylation (H3K27me3). Interplay between the two modulators influence lineage specification in stem cells. Here, we identified microRNA *MIR146A* to be a negative regulator of *JMJD3*. In the osteogenic differentiation of human mesenchymal stem cells (hMSCs), we observed an upregulation of *JMJD3* and a downregulation of *MIR146A*. Blocking JMJD3 activity in differentiating hMSCs reduced transcript levels of osteogenic gene *RUNX2*. H3K27me3 levels decreased at the *RUNX2* promoter during cell differentiation. Modulation of *MIR146A* levels in hMSCs altered *JMJD3* and *RUNX2* expression and affected osteogenic differentiation. We conclude that JMJD3 promotes osteogenesis in differentiating hMSCs, with *MIR146A* regulating *JMJD3*.

Keywords

stem cells; microRNA; *JMJD3*; *MIR146A*; osteogenesis; cell differentiation

1. Introduction

Posttranslational modifications of specific amino acids on histone tails, including methylation and acetylation, are major regulators of gene expression. During stem cell differentiation, histone modifications are highly dynamic [1]. In order for cell lineages to be properly established, methyl or acetyl groups are added, removed, or maintained on histone lysine residues at specific gene loci to allow for lineage-specific gene expression. The establishment and maintenance of methylated histone marks result from the balance of activity between histone methyltransferases and histone demethylases. The Polycomb

Correspondence should be addressed to: Christopher J. Payne, c-payne@northwestern.edu, Ann & Robert H. Lurie Children's Hospital of Chicago Research Center, 225 E. Chicago Ave., Box #211, Chicago, IL 60611 USA, Phone: +1 773 755 6316, Fax: +1 773 755 6593.

The authors declare no potential conflicts of interest.

Repressive Complex (PRC2) is a protein complex associated with gene silencing through the repressive H3K27me3 mark. Enhancer of zeste homolog 2 (EZH2) is the catalytic subunit of PRC2 [2]. Its activity is countered by lysine (K)-specific demethylase 6B (KDM6B), also known as jumonji domain containing 3 (JMJD3), a histone demethylase capable of removing methyl groups from H3K27me3 and promoting gene expression [3–7]. Changes in H3K27me3 distribution are integral to many types of cell fate transitions, including differentiation and oncogenesis. These changes are frequently accompanied by changes in *JMJD3* and *EZH2* expression [8–10]. Recently, *JMJD3* knockdown in mouse embryonic fibroblasts was shown to increase reprogramming efficiency in generating induced pluripotent stem cells, while *EZH2* knockdown decreased efficiency [11]. Collectively, these findings suggest that EZH2 generally promotes ‘stemness’ by acting on pathways associated with pluripotency, while JMJD3 generally maintains cells in a differentiated state by acting on genes and pathways associated with differentiation.

As *EZH2* and *JMJD3* play important roles in influencing cell fate, their expression is tightly regulated. The precise mechanisms that control their expression, however, remain poorly characterized. MicroRNAs are short non-coding RNAs that influence a large number of biological processes. *EZH2* is a target of numerous microRNAs, including *MIR101*, *MIR26A*, and *MIR214* [12–14]. While several microRNAs have been shown to target *JMJD3*, the functional consequences of these interactions have not been determined [15]. Disruption in the regulation of many of these microRNAs is associated with some cancers, suggesting that microRNAs may play an important role in regulating the balance of *EZH2* and *JMJD3* expression [16].

Human mesenchymal stem cells (hMSCs) are multipotent stem cells that can be derived from different sources including bone marrow, adipose tissue, and umbilical cord. *In vitro*, hMSCs differentiate into multiple lineages including osteoblasts, chondrocytes, and adipocytes [17]. While bone marrow-derived MSCs have traditionally been used to generate osteogenic cells *in vitro*, numerous studies have demonstrated that umbilical cord-derived MSCs also differentiate into osteoblasts under defined culture conditions [18]. Epigenetic regulation of histone marks is crucial for lineage specification of hMSCs [19–21]. Recently, it was shown that the inhibition of EZH2 activity through phosphorylation specifically promoted hMSC differentiation along the osteogenic lineage [22]. Additionally, JMJD3 promotes osteogenesis in human and mouse mesenchymal stem cells, as well as the odontogenic differentiation of dental mesenchymal stem cells [23–25]. This suggests that the opposing actions of EZH2 and JMJD3 may coordinate hMSC differentiation by regulating the expression of lineage-specific genes. However, the mechanisms regulating the expression of *EZH2* and *JMJD3* during osteogenic differentiation are unknown. In this current study, we discovered that *MIR146A* inhibits *JMJD3* expression through its interaction with the *JMJD3* 3′UTR. We used human umbilical cord-derived MSCs to examine how the relative expression of *MIR146A* and *JMJD3* influences stem cell fate decisions.

2. Materials and methods

2.1 Cell Culture

The work described in this article was carried out in accordance with *The Code of Ethics of the World Medical Association (Declaration of Helsinki) for experiments involving humans* (http://www.wma.net/en/30publications/10policies/b3/index.html), *EU Directive 2010/63/EU for animal experiments* (http://ec.europa.eu/environment/chemicals/lab_animals/legislation_en.htm), and *Uniform Requirements for manuscripts submitted to Biomedical journals* (http://www.icmje.org). Human umbilical cord-derived mesenchymal stem cells (hMSCs, ATCC® PCS-500-010) were obtained from the American Type Culture Collection (ATCC, Manassas, VA) and maintained in Dulbecco's Modified Eagle Medium supplemented with 10% fetal bovine serum (FBS) according to standard protocols. To induce osteogenic differentiation, hMSCs were cultured in Lonza's osteogenic cell culture media containing 0.5% ascorbic acid, 0.5% dexamethasone and 1% βglycerophosphate (proprietary culture media for which the disclosure of molarities is not permitted; Lonza, Walkersville, MD). For gene expression studies, cells were differentiated for three weeks. The extent of differentiation was assayed by measuring osteocalcin in the media by ELISA, according to manufacturer's instructions (Quidel, San Diego, CA). The P19 mouse cell line was maintained in Alpha Minimum Essential Medium supplemented with 10% FBS. Cells were visualized using brightfield optics on a Leica DMR-HC microscope. Images were captured using a QImaging Retiga 4000R camera and processed using Adobe software.

For transfections, hMSCs were re-plated 24 h before transfection. Pre-miR *MIR146A* and non-targeting control (NTC) mimics were purchased from Life Technologies (Grand Island, NY). *MIR146A* hairpin inhibitor and non-targeting control (NTC) were purchased from ThermoScientific (Wilmington, DE). Full length *JMJD3* expression construct, including the 3′ UTR, was obtained from Addgene (Cambridge, MA; cat #24167) [3]. Transfections were performed using Lipofectamine 2000 (Life Technologies). For RNA transfections, approximately 100 pmol of RNA was used. For vector and RNA co-transfections, hMSCs were transfected with 750 ng of either pCMV-*JMDJ3* or pCMV-empty vector together with 20 pmol *MIR146A* mimic. For transfections with multiple RNAs, 50 pmol of each RNA was used. At 24 h after transfection, the media was changed to osteogenic media. Transfection efficiency was, on average, found to be 64.7% ± 7.59, using a FAM-labeled NTC mimic (n=17 random fields of view, SEM). Following transfections, cells were differentiated for three weeks before RNA or protein was harvested. P19 cells were transfected using Lipofectamine 2000, 500 ng pMir-*JMJD3* Reporter or pMir-*JMJD3-mut* Reporter, 500 ng pMiR-REPORT β-galactosidase vector (Promega, Madison, WI), and 20 pmol mimic.

For JMJD3 inhibition, cells were treated with 10 μM GSK-J4 or vehicle control (0.02% DMSO). Cells were treated for 6 h before induction of differentiation.

2.2 Luciferase assays

A plasmid vector, pMirTarget, containing the 3′UTR of human *JMJD3* (*KDM6B*, NCBI Reference Sequence: NM_001080424.1) downstream of the luciferase gene coding region was purchased from Origene (Rockville, MD; cat #SC213659). We refer to this plasmid as

the pMir-*JMJD3* reporter. A second plasmid vector, in which two nucleotides within the putative *MIR146A* binding site of the *JMJD3* 3′UTR were changed (pMir-*JMJD3*-mut reporter), was also purchased from Origene (custom order). At 24 h after transfection, cells were harvested. Luciferase and β-galactosidase activities were measured using the appropriate enzyme assays, following the manufacturer's instructions (Promega). Luciferase activity was normalized to β-galactosidase activity.

2.3 Chromatin immunoprecipitation (ChIP)

The methods of Dahl and Collas were used with modifications [26]. Approximately 1×10^6 cells per chromatin shearing sample were fixed in 1% formaldehyde (v/v) for 8 min at room temperature. Chromatin was sheared using a BioRuptor™ NextGen sonicator (Diagenode, Liège, Belgium). Immunoprecipitation was performed on chromatin using either anti-H3K27me3 antibodies (cat #07-449; Millipore, Billerica, MA) or anti-IgG control antibodies (Cell Signaling, Danvers, MA). Genomic DNA was precipitated and amplified by quantitative real time PCR. Primers used for ChIP are shown in Supplementary Table 1. Protein enrichment was calculated as a percentage of input.

2.4 Real-time quantitative reverse transcription-PCR (qRT-PCR)

Total RNA was isolated from cells using the RNeasy kit (Qiagen, Valencia, CA). The quantity and quality of isolated RNA was determined using the NanoDrop 2000 Spectrophotometer (ThermoScientific). RNA was reverse transcribed into cDNA using random hexamer primers and M-MLV reverse transcriptase (New England Biolabs, Ipswich, MA). For qRT-PCR of transcripts, cDNA was mixed with Power SYBR Green PCR master mix (Applied Biosystems, Foster City, CA) and analyzed on an Applied Biosystems 7500 Fast Real-Time PCR system. Primers are shown in Supplementary Table 1. For microRNA analysis, total RNA was transcribed into cDNA using the TaqMan MicroRNA Reverse Transcription Kit (Life Technologies). MicroRNA-specific cDNA was then mixed with TaqMan Universal Master Mix (Life Technologies) and analyzed on an Applied Biosystems 7500 Fast Real-Time PCR system. Quantification of the fold change in gene expression was determined by the $\Delta\Delta C_t$ method.

2.5 Western blot analysis

Cells were harvested and resuspended in RIPA lysis buffer [50 mM Tris-HCl pH 8.0, 150 mM NaCl, 1% NP-40, 0.5% sodium deoxycholate, 0.1% SDS] containing protease and phosphatase inhibitors. Total protein was quantified using the *DC* protein assay (BioRad, Hercules, CA). 30 μg of total protein was separated by SDS-PAGE and transferred to polyvinylidene fluoride membranes. Blots were blocked in 5% milk and incubated overnight with anti-α-tubulin (cat #sc-5286; Santa Cruz Biotechnology, Santa Cruz, CA), anti-EZH2 (cat #E9085-02B; US Biological, Salem, MA), anti-JMJD3 (cat #07-1533; Millipore), anti-EZH2 phospo T487 (cat #ab109398; Abcam, Cambridge, MA), or anti-H3K27me3 (cat #07-449; Millipore). After washing, blots were incubated with horseradish peroxide-conjugated secondary antibodies for 1 h at room temperature. Blots were incubated with a chemiluminescent substrate, exposed to X-ray film, and developed. The full, uncropped

western blot of JMJD3 in undifferentiated and differentiating hMSCs is shown in Supplementary Fig. 1.

3. Results

3.1 Direct association of *MIR146A* with the human *JMJD3* 3′ UTR

In silico analysis using the microRNA binding site algorithm TargetScan predicted human *JMJD3* to be a target of numerous microRNAs, including *MIR146A* [27]. Previous work by our lab and others has shown mouse and human *MIR146A* to be tightly regulated during adult stem cell differentiation in multiple tissue types, including spermatogonia, megakaryocytes, erythrocytes, and macrophages [28–30]. As JMJD3 is an important regulator of differentiation, we wondered whether *MIR146A* targeted human *JMJD3 in vitro*. To test this, we cloned the *JMJD3* 3′ untranslated region (UTR) into a luciferase reporter vector. As a negative control, the predicted *MIR146A* binding site within the *JMJD3* 3′ UTR was mutated to alter the sequence by two nucleotides (Fig. 1A). These luciferase vectors were then co-transfected into P19 cells with a *MIR146A* mimic or a non-targeting control (NTC) mimic. We previously used P19 cells to validate the binding of mouse *Mir146a* to the 3′ UTR of the mediator complex subunit 1 and they serve as ideal cells for these assays [28]. Relative to the *JMJD3* reporter- and NTC mimic-transfected condition, cells receiving the *JMJD3* reporter with the *MIR146A* mimic exhibited a significantly lower amount of luciferase activity (Fig. 1B). Conversely, cells receiving a mutated form of the *JMJD3* reporter along with the *MIR146A* mimic did not differ from the control *JMJD3* reporter- and NTC mimic-transfected condition, but had a significantly higher amount of luciferase activity than the cells receiving the non-mutated *JMJD3* reporter with the *MIR146A* mimic (Fig. 1B). Collectively, these results demonstrate that *MIR146A* is able to inhibit gene expression in the presence of the *JMJD3* 3′UTR.

3.2 Downregulation of *MIR146A* during *in vitro* hMSC differentiation

To determine the functional relationship of *MIR146A* and *JMJD3* during cell differentiation, we next examined their relative expression levels in undifferentiated human umbilical cord-derived MSCs and in hMSCs differentiating down the osteogenic lineage. Standard protocols for inducing osteogenic differentiation over the course of three weeks were used. Differentiation was verified by measuring levels of osteocalcin in the cell media (Fig. 1C) and by observing morphological changes (Fig. 1D). Osteocalcin levels increased 2.29-fold in the differentiated hMSC cultures. We also measured transcript levels of runt related transcription factor 2 (*RUNX2*), a marker of osteogenic differentiation, and found that they increased 20.32-fold (Fig. 1E). We then measured *MIR146A* transcript levels. Relative to undifferentiated hMSCs, the differentiating cells exhibited a 3.61-fold decrease in *MIR146A* expression (Fig. 1F). *JMJD3* gene expression increased 3.89-fold in the differentiating hMSCs, while *EZH2* levels also increased 2.10-fold (Fig. 1E). We next examined the cells for changes in protein expression. hMSCs undergoing osteogenic differentiation exhibited an increase in both JMJD3 and EZH2 protein levels (Fig. 1G). There was also an increase in EZH2 specifically phosphorylated at Thr 487, a modification which disrupts the binding of EZH2 to components of PRC2, thereby inhibiting its function (Fig. 1G) [22]. Accordingly, differentiating hMSCs showed lower levels of H3K27me3, suggesting that the additional

EZH2 present was non-functional (Fig. 1G). Taken together, our results show that *MIR146A* is downregulated following hMSC differentiation. This is accompanied by a concurrent upregulation of *JMJD3* and a global decrease in H3K27me3. This suggests that an interaction between *MIR146A* and *JMJD3* may partially regulate the osteogenic differentiation potential of hMSCs.

3.3 JMJD3 promotes the osteogenic differentiation of hMSCs

Following our observation that JMJD3 protein levels increase during osteogenic differentiation, we next sought to determine its role in this process. We blocked JMJD3 activity using the specific functional inhibitor GSK-J4 [31]. Undifferentiated hMSCs were treated with either 10 μM GSK-J4 or vehicle control. After a 6 h treatment period, osteogenic differentiation was then induced. Relative to the control, hMSCs treated with GSK-J4 showed a significant decrease in *RUNX2* expression (1.67-fold, Fig. 2A), indicating that JMJD3 inhibition partially suppressed differentiation. These results suggest that JMJD3 promotes the osteogenic differentiation of hMSCs.

We next investigated whether H3K27me3 levels at the promoters of osteogenesis-related genes change when hMSCs differentiate into osteoblasts. We performed chromatin immunoprecipitation for H3K27me3 on both undifferentiated and differentiated hMSCs, and examined the promoter regions of bone morphogenetic protein 2 (*BMP2*), *SP7* (osterix; *OSX*) and *RUNX2*. *BMP2* promotes osteogenesis and is regulated by JMJD3, while *SP7* is an osteogenesis-specific transcription factor [25, 32]. For all three gene promoters, we saw a significant decrease in H3K27me3 enrichment in differentiated cells compared to undifferentiated hMSCs (Fig. 2B). Importantly, we did not see a change in H3K27me3 enrichment at the *GAPDH* promoter. As an additional control, we examined downstream regions of the *RUNX2* and *SP7* genes for changes in H3K27me3 levels between undifferentiated and differentiating hMSCs. We did not see altered enrichment (Supplementary Fig. 2). Collectively, these findings support the hypothesis that JMJD3 activity regulates the expression of genes required for osteogenesis through a decrease in H3K27me3 levels at their promoters.

3.4 *MIR146A* expression modulates hMSC differentiation into osteoblasts

We next determined the biological effect of overexpressing *MIR146A* during *in vitro* hMSC differentiation. hMSCs were transfected with either a *MIR146A* mimic or an NTC mimic immediately before inducing osteogenic differentiation. We then examined the transcript levels of *EZH2*, *JMJD3*, and *RUNX2* in both NTC mimic-transfected and *MIR146A*-transfected cells. While there was no significant change in *EZH2* expression upon *MIR146A* overexpression relative to NTC, *MIR146A*-transfected cells showed significant decreases in both *JMJD3* (3.02-fold) and *RUNX2* (22.08-fold) (Fig. 3A). We also measured protein levels in the transfected cells. hMSCs overexpressing *MIR146A* exhibited a decrease in JMJD3 and an increase in H3K27me3 (Fig. 3B). Unexpectedly, we saw a slight increase in EZH2 levels in *MIR146A*-transfected cells. This suggests that EZH2 may be regulated by a mechanism independent of *MIR146A*. To confirm that the effects of the *MIR146A* mimic were specific, we treated hMSCs simultaneously with a *MIR146A* mimic and a *MIR146A* hairpin inhibitor or an NTC inhibitor before inducing cell differentiation. Co-treatment with

the *MIR146A* inhibitor was expected to relieve the effects of the *MIR146A* mimic and allow the cells to differentiate normally. Relative to hMSCs receiving the *MIR146A* mimic and NTC inhibitor, hMSCs receiving both the *MIR146A* mimic and *MIR146A* inhibitor exhibited an upregulation of *JMJD3* (9.85-fold) and *RUNX2* (2.46-fold) (Supplementary Fig. 3). We conclude that our *MIR146A* overexpression experiments are specific and that they do not induce off-target effects.

We next examined the impact of *MIR146A* inhibition on osteogenic differentiation. hMSCs were transfected with a *MIR146A* inhibitor or NTC inhibitor immediately before the induction of osteogenic differentiation. Inhibition of *MIR146A* significantly increased the expression of *JMJD3* (3.57-fold) and *RUNX2* (5.40-fold) (Fig. 3C). There was no effect on the transcript levels of *EZH2*, further evidence that *EZH2* is not regulated by *MIR146A*. These results demonstrate that changes in *MIR146A* expression in differentiating hMSCs modulate the levels of key transcripts and proteins fundamental to osteogenic differentiation. Finally, we wanted to confirm that the biological impact of *MIR146A* on osteogenic differentiation was specifically mediated through *JMJD3*. We modulated *JMJD3* expression levels in hMSCs by transfecting them with a *JMJD3* expression vector or a control vector together with a *MIR146A* mimic for 24 h [3]. Osteogenic differentiation was then induced. By the end of the differentiation period, cells receiving the *JMJD3* plasmid vector in the presence of the *MIR146A* mimic exhibited a significant increase in the expression of both *RUNX2* (2.51-fold, Fig. 3D), and *JMJD3* (1,069-fold, Fig. 3D), whose high levels were likely due to both the constitutive expression of the vector and the endogenous expression induced during the differentiation process. These findings indicate that *JMJD3* overexpression alleviates the effects of elevated *MIR146A* levels in the cells, and suggest that the impact of *MIR146A* on hMSC differentiation is specifically due to its regulation of *JMJD3*.

4. Discussion

Multipotent MSCs generate distinct cell types within the mesenchymal lineage, including bone, cartilage, and fat [17]. It has become clear in recent years that microRNAs are major regulators of MSC differentiation, and that they can promote, as well as inhibit, distinct MSC differentiation pathways [33–36]. In this study, we have identified an inhibitory role for *MIR146A* in regulating the osteogenic differentiation potential of hMSCs. *MIR146A* has previously been shown by our group and others to be highly expressed in multiple types of adult stem cells, and to play a role in regulating cell differentiation [28–30]. Collectively, these findings suggest that *MIR146A* may be linked to cell differentiation signaling mechanisms. Our current finding that *MIR146A* is an inhibitor of *JMJD3* expression supports this hypothesis. To determine how *MIR146A* fits into the regulatory network of stem cell differentiation, more work is needed to decipher the control of its expression during differentiation processes.

A major feature of MSC differentiation is the extensive chromatin remodeling that occurs upon commitment of the cells to differentiate [19–21]. A recent study found that in adipose-derived MSCs, lineage specific promoters lost enrichment of H3K27me3 upon differentiation [37]. When late passage cells that had lost differentiation potential were

induced to differentiate, they showed a dramatic upregulation of EZH2 and retained H3K27me3 at specific adipogenic gene promoters [37]. This suggests that the loss of H3K27me3 enrichment at specific genes is required for the progression of differentiation. In support of this, JMJD3 has been shown to be an important regulator of stem cell differentiation. In mouse neural stem cells and human keratinocytes, differentiation leads to an increase in JMJD3 expression, concurrent with the loss of H3K27me3 marks at genes important for differentiation progression [9, 38]. During MSC senescence, JMJD3 expression increases, while PRC2 expression decreases [39]. MSC lineage specification is accompanied by dramatic epigenetic remodeling, including changes to PRC2 expression and global H3K27me3 distribution. Here, we have shown that *JMJD3* transcript and protein expression increases significantly during hMSC differentiation. A role for *JMJD3* in osteogenesis has also been shown previously in human and mouse MSCs through its removal of H3K27me3 marks from key osteogenic genes [23–25]. Collectively, this evidence supports the hypothesis that *JMJD3* upregulation in differentiating hMSCs ensures that key remodeling events can occur throughout the differentiation process. In this manner, *MIR146A* inhibition of *JMJD3* might prevent early differentiation in uncommitted hMSCs. Despite its involvement in many cellular processes, little is known about how *JMJD3* expression is regulated. To our knowledge, this report is the first to describe a post-transcriptional regulatory mechanism of JMJD3 control during cell differentiation by a microRNA. Further investigation into the regulation of *JMJD3* expression will increase our understanding of JMJD3 function and how it counters the activity of EZH2.

Supplementary Material

Refer to Web version on PubMed Central for supplementary material.

Acknowledgments

The authors thank Kristin Kalita for her contribution towards identifying *MIR146A* as a target of *JMJD3* in preliminary experiments, and Dr. Jenny Kerschner for her careful review of the manuscript. We gratefully acknowledge the Children's Research Fund of the Ann & Robert H. Lurie Children's Hospital of Chicago Research Center for its generous financial support. C.J.P. is the recipient of an NIH Pathway-to-Independence Award from the Eunice Kennedy Shriver National Institute of Child Health and Human Development (R00 HD055330).

Abbreviations

EZH2	enhancer of zeste homolog 2
H3K27me3	histone H3 lysine 27 trimethylation
hMSCs	human mesenchymal stem cells
JMJD3	jumonji domain containing 3
PRC2	Polycomb Repressive Complex 2
RUNX2	runt related transcription factor 2
3′ UTR	3′ untranslated region

References

1. Tollervey JR V, Lunyak V. Epigenetics: judge, jury and executioner of stem cell fate. Epigenetics. 2012; 7(8):823–40. [PubMed: 22805743]
2. Margueron R, Reinberg D. The Polycomb complex PRC2 and its mark in life. Nature. 2011; 469(7330):343–9. [PubMed: 21248841]
3. Agger K, et al. UTX and JMJD3 are histone H3K27 demethylases involved in HOX gene regulation and development. Nature. 2007; 449(7163):731–4. [PubMed: 17713478]
4. De Santa F, et al. The histone H3 lysine-27 demethylase Jmjd3 links inflammation to inhibition of polycomb-mediated gene silencing. Cell. 2007; 130(6):1083–94. [PubMed: 17825402]
5. Hong S, et al. Identification of JmjC domain-containing UTX and JMJD3 as histone H3 lysine 27 demethylases. Proc Natl Acad Sci U S A. 2007; 104(47):18439–44. [PubMed: 18003914]
6. Lan F, et al. A histone H3 lysine 27 demethylase regulates animal posterior development. Nature. 2007; 449(7163):689–94. [PubMed: 17851529]
7. Xiang Y, et al. JMJD3 is a histone H3K27 demethylase. Cell Res. 2007; 17(10):850–7. [PubMed: 17923864]
8. Jepsen K, et al. SMRT-mediated repression of an H3K27 demethylase in progression from neural stem cell to neuron. Nature. 2007; 450(7168):415–9. [PubMed: 17928865]
9. Sen GL, et al. Control of differentiation in a self-renewing mammalian tissue by the histone demethylase JMJD3. Genes Dev. 2008; 22(14):1865–70. [PubMed: 18628393]
10. Agger K, et al. The H3K27me3 demethylase JMJD3 contributes to the activation of the INK4A-ARF locus in response to oncogene- and stress-induced senescence. Genes Dev. 2009; 23(10): 1171–6. [PubMed: 19451217]
11. Zhao W, et al. Jmjd3 Inhibits Reprogramming by Upregulating Expression of INK4a/Arf and Targeting PHF20 for Ubiquitination. Cell. 2013; 152(5):1037–50. [PubMed: 23452852]
12. Varambally S, et al. Genomic loss of microRNA-101 leads to overexpression of histone methyltransferase EZH2 in cancer. Science. 2008; 322(5908):1695–9. [PubMed: 19008416]
13. Wong CF, Tellam RL. MicroRNA-26a targets the histone methyltransferase Enhancer of Zeste homolog 2 during myogenesis. J Biol Chem. 2008; 283(15):9836–43. [PubMed: 18281287]
14. Derfoul A, et al. Decreased microRNA-214 levels in breast cancer cells coincides with increased cell proliferation, invasion and accumulation of the Polycomb Ezh2 methyltransferase. Carcinogenesis. 2011; 32(11):1607–14. [PubMed: 21828058]
15. Ichi S, et al. Folic Acid Remodels Chromatin on Hes1 and Neurog2 Promoters during Caudal Neural Tube Development. Journal of Biological Chemistry. 2010; 285(47):36922–36932. [PubMed: 20833714]
16. Benetatos L, et al. Non-coding RNAs and EZH2 interactions in cancer: Long and short tales from the transcriptome. Int J Cancer. 2012
17. Pittenger MF, et al. Multilineage potential of adult human mesenchymal stem cells. Science. 1999; 284(5411):143–7. [PubMed: 10102814]
18. Lee OK, et al. Isolation of multipotent mesenchymal stem cells from umbilical cord blood. Blood. 2004; 103(5):1669–75. [PubMed: 14576065]
19. Tan J, et al. Genome-wide analysis of histone H3 lysine9 modifications in human mesenchymal stem cell osteogenic differentiation. PLoS One. 2009; 4(8):e6792. [PubMed: 19710927]
20. Collas P. Programming differentiation potential in mesenchymal stem cells. Epigenetics. 2010; 5(6):476–82. [PubMed: 20574163]
21. Karpiuk O, et al. The histone H2B monoubiquitination regulatory pathway is required for differentiation of multipotent stem cells. Mol Cell. 2012; 46(5):705–13. [PubMed: 22681891]
22. Wei Y, et al. CDK1-dependent phosphorylation of EZH2 suppresses methylation of H3K27 and promotes osteogenic differentiation of human mesenchymal stem cells. Nat Cell Biol. 2011; 13(1): 87–94. [PubMed: 21131960]
23. Xu J, et al. KDM6B epigenetically regulates odontogenic differentiation of dental mesenchymal stem cells. Int J Oral Sci. 2013; 5(4):200–5. [PubMed: 24158144]

24. Yang D, et al. Histone demethylase Jmjd3 regulates osteoblast differentiation via transcription factors Runx2 and osterix. J Biol Chem. 2013; 288(47):33530–41. [PubMed: 24106268]
25. Ye L, et al. Histone demethylases KDM4B and KDM6B promotes osteogenic differentiation of human MSCs. Cell Stem Cell. 2012; 11(1):50–61. [PubMed: 22770241]
26. Dahl JA, Collas P. Q2ChIP, a quick and quantitative chromatin immunoprecipitation assay, unravels epigenetic dynamics of developmentally regulated genes in human carcinoma cells. Stem Cells. 2007; 25(4):1037–46. [PubMed: 17272500]
27. Lewis BP, Burge CB, Bartel DP. Conserved seed pairing, often flanked by adenosines, indicates that thousands of human genes are microRNA targets. Cell. 2005; 120(1):15–20. [PubMed: 15652477]
28. Huszar JM, Payne CJ. MicroRNA 146 (Mir146) modulates spermatogonial differentiation by retinoic acid in mice. Biol Reprod. 2013; 88(1):15. [PubMed: 23221399]
29. Starczynowski DT, et al. MicroRNA-146a disrupts hematopoietic differentiation and survival. Exp Hematol. 2011; 39(2):167–178 e4. [PubMed: 20933052]
30. Labbaye C, et al. A three-step pathway comprising PLZF/miR-146a/CXCR4 controls megakaryopoiesis. Nat Cell Biol. 2008; 10(7):788–801. [PubMed: 18568019]
31. Kruidenier L, et al. A selective jumonji H3K27 demethylase inhibitor modulates the proinflammatory macrophage response. Nature. 2012; 488(7411):404–8. [PubMed: 22842901]
32. Nakashima K, et al. The novel zinc finger-containing transcription factor Osterix is required for osteoblast differentiation and bone formation. Cell. 2002; 108(1):17–29. [PubMed: 11792318]
33. Inose H, et al. A microRNA regulatory mechanism of osteoblast differentiation. Proc Natl Acad Sci U S A. 2009; 106(49):20794–9. [PubMed: 19933329]
34. Li Z, et al. A microRNA signature for a BMP2-induced osteoblast lineage commitment program. Proc Natl Acad Sci U S A. 2008; 105(37):13906–11. [PubMed: 18784367]
35. Yang B, et al. MicroRNA-145 regulates chondrogenic differentiation of mesenchymal stem cells by targeting Sox9. PLoS One. 2011; 6(7):e21679. [PubMed: 21799743]
36. Bengestrate L, et al. Genome-wide profiling of microRNAs in adipose mesenchymal stem cell differentiation and mouse models of obesity. PLoS One. 2011; 6(6):e21305. [PubMed: 21731698]
37. Noer A, Lindeman LC, Collas P. Histone H3 modifications associated with differentiation and long-term culture of mesenchymal adipose stem cells. Stem Cells Dev. 2009; 18(5):725–36. [PubMed: 18771397]
38. Sola S, et al. p53 interaction with JMJD3 results in its nuclear distribution during mouse neural stem cell differentiation. PLoS One. 2011; 6(3):e18421. [PubMed: 21483786]
39. Jung JW, et al. Histone deacetylase controls adult stem cell aging by balancing the expression of polycomb genes and jumonji domain containing 3. Cell Mol Life Sci. 2010; 67(7):1165–76. [PubMed: 20049504]

Highlights

- Human *JMJD3* is a direct target of *MIR146A*
- Differentiating hMSCs downregulate *MIR146A* and upregulate *JMJD3* and *RUNX2*
- *MIR146A* overexpression in differentiating hMSCs inhibits *JMJD3* and *RUNX2*
- H3K27me3 levels decrease at the *RUNX2* promoter in differentiating hMSCs
- We conclude that *MIR146A* negatively regulates *JMJD3* in undifferentiated hMSCs

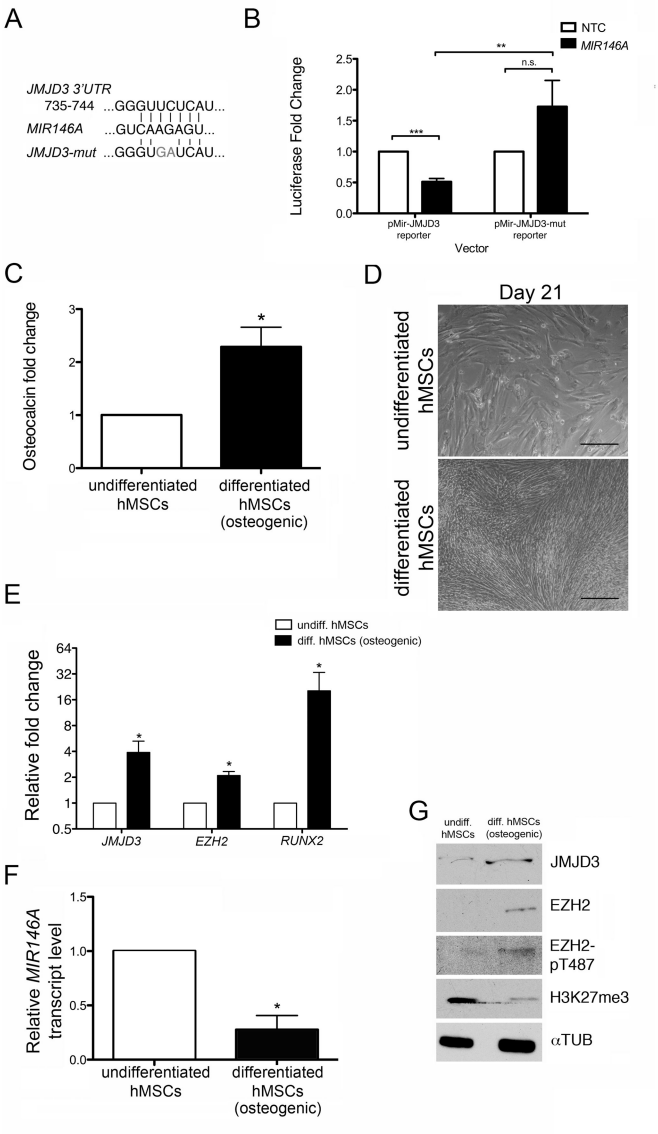

Figure 1. *MIR146A* targets *JMJD3* and is downregulated during hMSC differentiation

(A) The nucleotide sequence of the *MIR146A* binding site within the *JMJD3* 3′UTR. A mutated version of the binding site (‘*JMJD3*-mut’) served as a negative control. (B) Plasmid vectors containing the luciferase gene coding region upstream of either the *JMJD3* 3′UTR (pMir-*JMJD3* reporter) or the *JMJD3*-mut 3′UTR (pMir-*JMJD3*-mut reporter) were cotransfected with a *MIR146A* mimic or a non-targeting control (NTC) mimic into P19 cells. The fold change in luciferase activity following *MIR146A* transfection is shown relative to NTC transfection. (C) Osteocalcin concentration in the cell media was measured by ELISA. Relative osteocalcin levels are depicted as a fold change in differentiated hMSCs relative to undifferentiated hMSCs. (D) Brightfield images of undifferentiated (top) and differentiated (bottom) hMSCs at the end of a 21-day differentiation period. Scale bars = 40 μM. (E) Fold change in qRT-PCR transcripts of *JMJD3*, *EZH2*, and *RUNX2* in differentiating hMSCs relative to undifferentiated hMSCs. All transcripts were normalized to *GAPDH*. (F) qRT-

PCR of *MIR146A* in undifferentiated and differentiating hMSCs. *MIR146A* transcript levels were normalized to *U6* snRNA. (G) Representative western blot showing protein levels of JMJD3, EZH2, EZH2-pT487, and H3K27me3. αTUB was used as a loading control. All graphs (B, C, E, F) exhibit the mean value ± SEM of 3 biological replicates. **P*<0.05, ****P*<0.001; statistical differences were calculated by Student's t test.

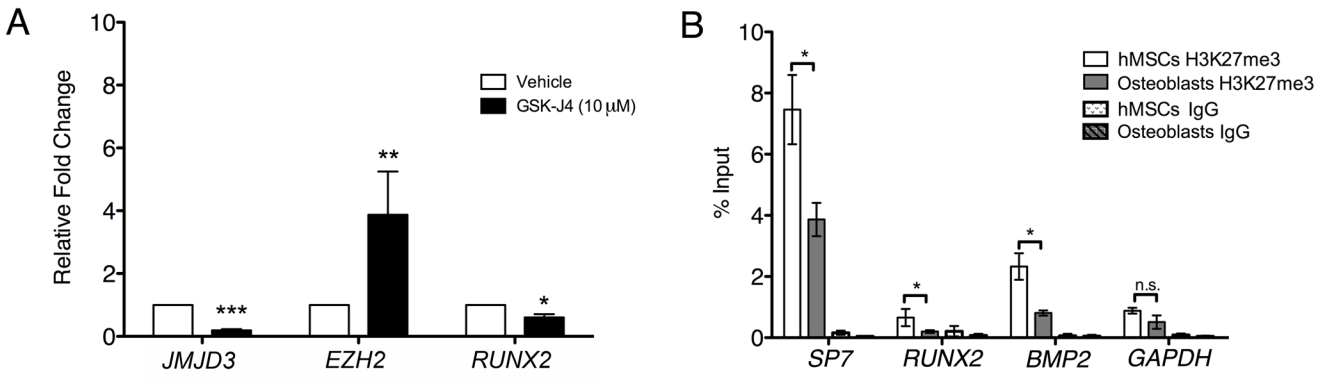

Figure 2. *JMJD3* promotes osteogenic differentiation of hMSCs by regulating osteogenic transcription factors

(A) qRT-PCR of *EZH2*, *JMJD3*, and *RUNX2* following differentiation of hMSCs treated with either JMJD3 inhibitor GSK-J4 or 0.02% DMSO. The fold change in transcript levels following GSK-J4 treatment is shown relative to vehicle treatment. (B) Promoter regions of *SP7*, *RUNX2*, *BMP2*, and *GAPDH* were examined by ChIP using either anti-H3K27me3 antibody or anti-IgG control antibody. Enrichment is presented as percent of chromatin input. All graphs exhibit the mean value ± SEM of 3 biological replicates. **P*<0.05, ***P*<0.01, ****P*<0.001; statistical differences were calculated by Student's t test.

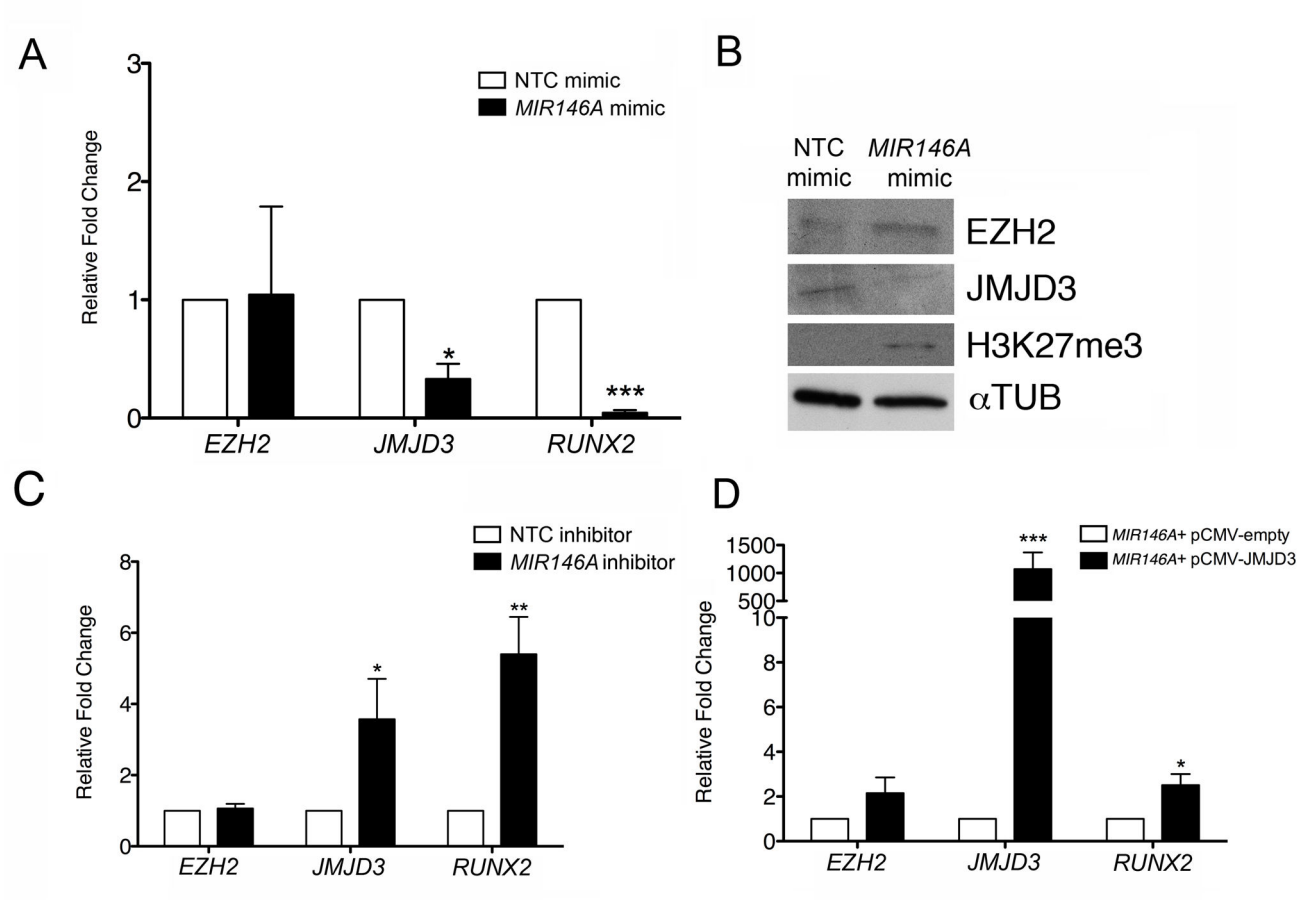

Figure 3. Modulation of *MIR146A* in hMSCs impacts osteogenic differentiation

(A) Fold change in qRT-PCR transcripts of *EZH2*, *JMJD3*, and *RUNX2* in *MIR146A* mimic-transfected hMSCs relative to NTC mimic-transfected hMSCs. All transcripts were normalized to *GAPDH*. (B) Representative western blot depicting levels of EZH2, JMJD3, and H3K27me3 in NTC mimic- and *MIR146A* mimic-transfected cells. αTUB was used as a loading control. (C) Fold change in qRT-PCR transcripts of *EZH2*, *JMJD3*, and *RUNX2* in *MIR146A* inhibitor-transfected hMSCs relative to NTC inhibitor-transfected hMSCs. All transcripts were normalized to *GAPDH*. (D) Fold change in qRT-PCR transcripts of *EZH2*, *JMJD3*, and *RUNX2* in differentiated hMSCs transfected with *MIR146A* mimic + *JMJD3* expression construct pCMV-JMJD3 relative to differentiated hMSCs transfected with *MIR146A* mimic + control pCMV empty vector. All transcripts were normalized to *GAPDH*. All graphs (A, C, D) exhibit the mean value ± SEM of 3 biological replicates. **P*<0.05, ***P*<0.01, ****P*< 0.001; statistical differences were calculated by Student's t test.